Molecular Therapy
Nucleic Acids
Original Article

Comprehensive RNA-seq reveals molecular changes in kidney malignancy among people living with HIV

Juan Bao,[1,6] Jianqing Ye,[2,3,6] Jingjing Xu,[1,6] Shanshan Liu,[1] Lin Wang,[1] Zehuan Li,[4] Qiuyue Li,[1] Feng Liu,[1] Xiaomeng He,[1] Heng Zou,[1] Yanling Feng,[1] Christopher Corpe,[5] Xiaoyan Zhang,[1] Jianqing Xu,[1] Tongyu Zhu,[1] and Jin Wang[1]

[1]Shanghai Public Health Clinical Center, Fudan University, 2901 Caolang Road, Jinshan District, Shanghai 201508, China; [2]Department of Urology, Xinhua Hospital, School of Medicine, Shanghai Jiaotong University, 1665 Kongjiang Road, Shanghai, China; [3]Department of Urology, The Third Affiliated Hospital of Second Military Medical University, Shanghai, China; [4]Department of General Surgery, Zhongshan Hospital, Fudan University, Shanghai, China; [5]King's College London, London, Nutritional Science Department, 150 Stamford Street, Waterloo, London SE19NH, UK

To heighten the awareness of kidney malignancy in patients with HIV infection to facilitate the early diagnosis of kidney cancer, the differentially expressed mRNAs were analyzed in this malignant tumor using RNA sequencing. We identified 2,962 protein-coding transcripts in HIV-associated kidney cancer. KISS1R, CAIX, and NPTX2 mRNA expression levels were specifically increased in HIV-associated kidney cancer while UMOD and TMEM213 mRNA were decreased in most cases based on real-time PCR analyses. These findings were similar to those noted for the general population with renal cell carcinoma. Immunohistochemical staining analysis also showed that a total of 18 malignant kidney cases among the people living with HIV (PLWH) exhibited positive staining for KISS1R and CAIX. Pathway analysis of the differentially expressed mRNAs in HIV-associated kidney cancer revealed that several key pathways were involved, including vascular endothelial growth factor-activated receptor activity, IgG binding, and lipopolysaccharide receptor activity. Altogether, our findings reveal the identified molecular changes in kidney malignancy, which may offer a helpful explanation for cancer progression and open up new therapeutic avenues that may decrease mortality after a cancer diagnosis among PLWH.

INTRODUCTION

Since the introduction of highly active antiretroviral therapy (HAART) in the last two decades, human immunodeficiency virus (HIV)-infected individuals have a significantly reduced incidence of AIDS-related morbidity at the cost of a higher risk for developing certain cancers[1–3] and individuals with non-AIDS-defining cancers (NADCs) have a worse prognosis than the general population.[4] Moreover, NADC has already become one of the top causes of non-AIDS-related death among patients living with HIV.[5,6]

Kidney disease is the fourth-leading cause of death in people living with HIV (PLWH) in the United States and has become an increasingly important cause of patient morbidity and mortality.[7,8] The native kidney is a reservoir for HIV-1 and can maintain the ability of the virus to persist and produce viral antigens and/or new virions involved in HIV pathogenesis.[9] The presence of HIV in kidney cells can manifest itself in various ways, including indolent nephropathy, inflammation, and proteinuria with glomerular abnormalities.[10] HIV-positive patients are at increased risk for kidney diseases, such as HIV-associated nephropathy (HIVAN), noncollapsing focal segmental glomerulosclerosis, immune-complex kidney disease, comorbid kidney disease, and kidney injury resulting from prolonged exposure to antiretroviral therapy (ART).[11] Zhang et al. recently found that the clinical characteristics, treatment measures, and pathology of 19 HIV-positive renal cell carcinoma (RCC) patients were similar to those of the general population.[12] Although similar to RCC, HIV-associated kidney cancer has a poor prognosis in an advanced stage and is difficult to detect early due to the lack of molecular biomarkers[13] and the incidence of RCC in the HIV-positive population is greater than that in the non-HIV population.[14,15] In a large meta-analysis of seven population-based HIV cancer studies involving more than 400,000 HIV-positive patients, Grulich et al. reported a standardized incidence ratio of 1.50 for RCC in the HIV-positive population.[14]

Although no clear relationship between the degree of immunosuppression and the risk of kidney cancer has been defined, genetic alterations along with dysregulation of epigenetic pathways of HIV-associated kidney cancer are involved in its tumorigenesis as a heterogeneous disease.[16] Genomic analysis yielded millions of protein-coding transcripts and noncoding RNAs that participate in virtually all cancer cellular

Received 21 November 2021; accepted 5 June 2022;
https://doi.org/10.1016/j.omtn.2022.06.002.

[6]These authors contributed equally

Correspondence: Jin Wang, Shanghai Public Health Clinical Center, Fudan University, 2901 Caolang Road, Jinshan District, Shanghai 201508, China.
E-mail: wjincityu@yahoo.com

Table 1. Clinicopathological characteristics of 18 patients with HIV-associated kidney cancer

		Overall survival	
Clinicopathological characteristic	No. of patients	Months ± SD	p value
Age (years)			0.307
<60	12	28.08 ± 20.46	
≥60	6	17.83 ± 16.88	
Gender			0.313
Female	1	5.00 ± 0.00	
Male	17	25.82 ± 19.43	
Smoking[a]			0.663
+	3	29.33 ± 32.81	
–	15	23.73 ± 17.36	
HAART			0.329
+	15	22.60 ± 19.20	
–	3	35.00 ± 21.28	
$CD4^+$ count			0.399
<200	2	36.00 ± 43.84	
>200	16	23.25 ± 16.81	
Complication[a]			**0.023**
+	5	8.40 ± 3.29	
–	13	30.92 ± 19.53	
Surgical approach[a]			**0.019**
Open radical	13	31.08 ± 19.31	
Laparoscopic radical	5	8.00 ± 3.74	
Pathological type[b]			0.205
Clear cell renal cell carcinoma	13	27.38 ± 19.75	
Papillary renal cell carcinoma	3	8.33 ± 3.06	
Nephroblastoma	1	51.00 ± 0.00	
Squamous cell carcinoma	1	12.00 ± 0.00	
TMN stage			0.175
I–II	8	31.75 ± 26.41	
III–IV	10	19.00 ± 9.71	

[&]Complication (−): patient without syphilis/hypertension/coronary heart disease/diabetes/hepatitis B.
*The significant differences in survival outcome were noted between groups based on pairwise comparison analysis ($p \leq 0.05$).
[a]Smoking (−): never smoked.
[b]No significant differences in survival outcome were noted between groups based on pairwise comparison analysis among pathological types of HIV-associated renal cell carcinoma.

processes, demonstrating that a spectrum of diverse genomic alterations can define renal carcinoma subtypes in the general population with RCC.[17] To improve treatment, provide information about the course of cancer, and predict response to chemotherapy, genome-wide expression studies may provide an unbiased approach for investigating the mechanisms of kidney carcinogenesis in HIV infection and molecularly defining this cancer. In this report, we employ a comprehensive RNA sequencing (RNA-seq) analysis of six HIV-associated kidney tumor/adjacent normal tissue samples.

RESULTS

Baseline characteristics

Of the 4,027 HIV-positive patients managed by the Shanghai Public Health Clinical Center between March 2014 and June 2019, 18 patients with a diagnosis of RCC were identified, as shown in Table 1, which summarizes the baseline characteristics of the patients with RCC. Among the 18 patients with HIV-associated kidney cancer enrolled in the study, the age of patients with kidney cancer ranged from 24 to 65 years and the average age was 51.72 ± 12.15 years. Fifteen of the 18 patients were on ART at the time of RCC diagnosis. Four patients with HIV-associated kidney cancer had histories of comorbidities, such as syphilis or tuberculosis. A total of 8 patients were identified with stage I–II kidney cancer and 10 patients were identified with stage III–IV kidney cancer, including 13 patients with clear cell renal cell carcinoma (ccRcc) 3 patients with papillary RCC (PRCC), 1 patient with nephroblastoma, 1 patient with squamous cell carcinoma (SCC), and 1 patient with perivascular epithelioid cell tumor. Univariate analysis by SPSS showed that overall survival (OS) did not differ by age, sex, smoking, HAART treatment, $CD4^+$ count, pathological type, or TNM stage among these patients. The median OS duration of the 18 patients was 18.50 months. However, significant differences in survival outcomes were noted between patients without syphilis/hypertension/coronary heart disease/diabetes/hepatitis (30.92 ± 19.53 months) and patients with complications (8.40 ± 3.29 months) ($p = 0.023$). Specifically, patients with complications were associated with decreased OS duration, an open radical surgical approach (31.08 ± 19.31 months), and an arthroscopic radical surgical approach (8.00 ± 3.74 months) ($p = 0.019$) (Table 1).

Analysis of RNA-seq data and transcriptomic profiles in HIV-associated kidney cancer

During the amplification step of sequence generation, the Illumina NovaSeq 6000 produces clusters of identical sequence fragments. The number of these clusters is reported and the percentage of sequence fragments that pass quality filtering by the Illumina image analysis software is also reported. Across all 6 samples, the total number of reads produced for each sample ranged from 35,739,250 to 51,931,536 with a median of 41,010,336, and 97.61%–99.07% of reads were aligned to the reference genome (Table S2). No significant difference in the number of reads from adjacent normal tissue and HIV-associated kidney tumor tissue was noted ($p = 0.175$). RNA sequencing analysis identified 2,962 protein-coding transcripts, 131 pseudogenes, and 39 novel transcripts that exhibited a greater than a 2.0-fold change in expression level ($p \leq 0.05$) in the HIV-associated kidney cancer and adjacent normal tissue groups. These differentially expressed genes (DEGs) are included in a volcano plot in Figure 1A. The heatmap shows that clusters of genes share similar expression patterns at the transcript levels of these DEGs (Figure 1B) in HIV-associated kidney cancer. Moreover, we identified 652 DEGs (Table 2) with a 5.0-fold change in expression level ($Q \leq 0.05$) in HIV-associated kidney cancer. Furthermore, using The Cancer Genome Atlas (TCGA) data of multiple cancer types for the analysis of 652 DEGs in HIV-associated kidney cancer, we identified nine DEGs (CAMK2A, STC2,

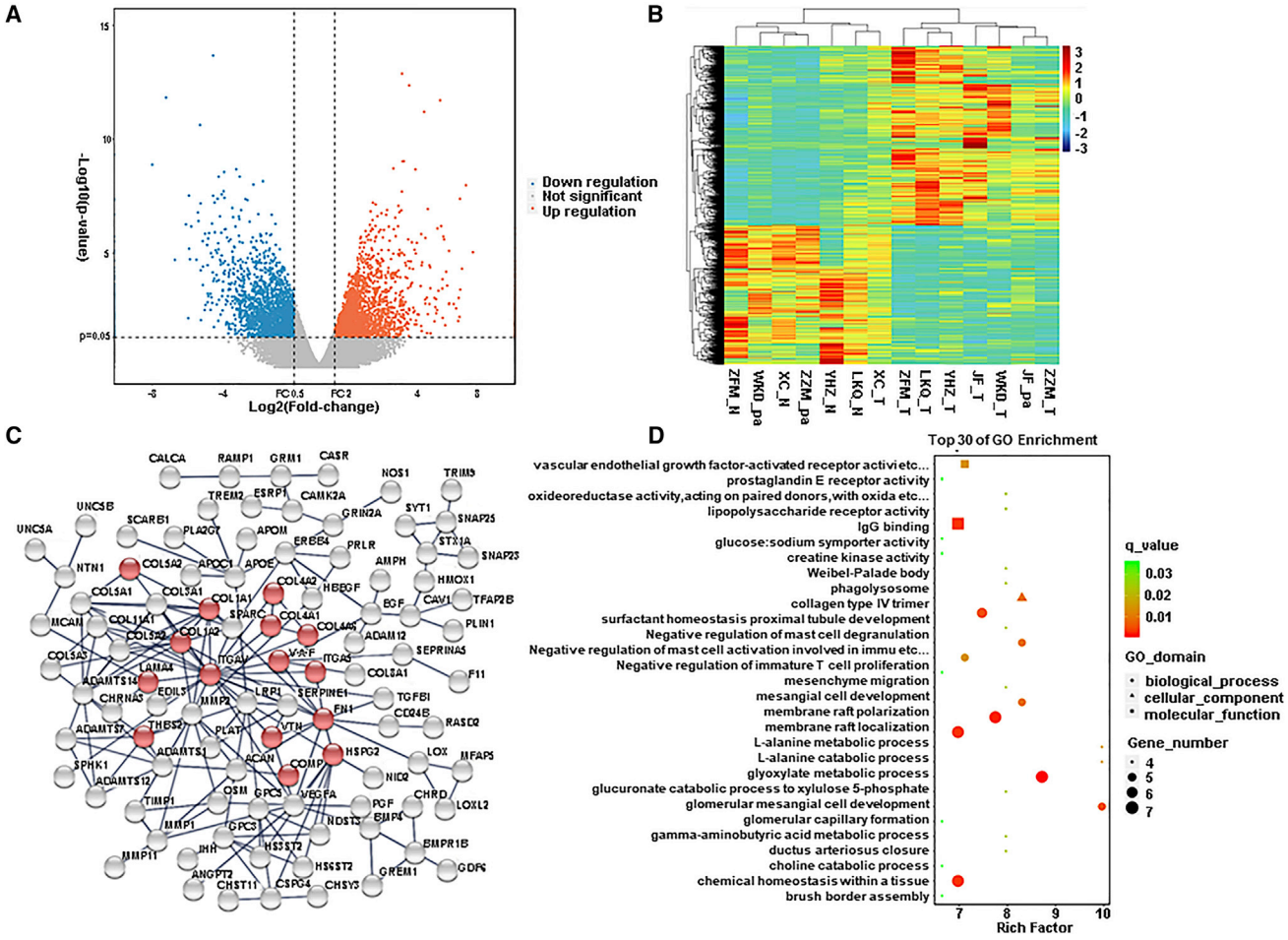

Figure 1. Volcano plot , heatmap , protein-protein interaction and functional enrichment analyses of mRNAs expression

Analysis of significantly expressed genes in HIV-associated kidney cancer, which are shown in a volcano plot (A) and based on hierarchical clustering (B), protein-protein interaction analysis (C), and functional enrichment analyses of mRNAs. (D) Functional network analyses were in HIV-associated kidney cancer. Compared with adjacent normal tissue groups, significantly highly expressed genes in HIV-associated kidney cancer were defined as genes with a fold change $\geq$2.0, p $\leq$ 0.05, shown in red; significantly less expressed genes are shown in blue with a fold change $\leq$0.5, p value $\leq$0.05; genes that did not meet the criteria are shown in gray; upregulated DEGs are shown in red, and downregulated DEGs are shown in green in the volcano plot (A).

FAM153CP, COL23A1, DPYSL3, PCDHB1, PCDHGC4, SH3PXD2B, and SPARC) that had a high incidence of genetic alterations in kidney renal clear cell carcinoma (TCGA-Nature 2013, 5.1%–6.9%; TCGA-Firehose Legacy, 14.6%–16.8%) with an incidence cutoff value of $\geq$5.0% in the two kidney cancer TCGA lists that included 838 patients. These genes were also significantly frequently altered across cancer types, including breast invasive carcinoma (1.1%–6.5%), bladder urothelial carcinoma (2.4%–10.0%), and lung adenocarcinoma (0.4%–7.4%) (Table 3). Our analysis suggests that alterations in the nine DEGs (CAMK2A, STC2, FAM153CP, COL23A1, DPYSL3, PCDHB1, PCDHGC4, SH3PXD2B, and SPARC) are important in at least a subset of tumors. A strong tendency of co-occurrences was also noted for genetic alterations in the DEGs ($p < 0.001$) in Table S3. Considering the regulatory role of these nine candidate genes, the underlying mechanisms and cellular consequences of these interactions could be critical for understanding HIV-associated kidney cancer pathology.

Protein-protein interaction and functional pathway analysis of HIV-associated kidney cancer

To further elucidate the regulatory and interaction relationships, 652 DEGs were imported into the STRING database. The STRING database identified a network of 503 mRNAs and 595 edges (interaction relationships). The 15 mRNAs (ITGAV, ITGA5, VWF, FN1, VTN, HSPG2, COMP, THBS2, LAMA4, COL1A1, COL1A2, COL4A1, COL4A2. COL4A6, and COL6A2) in the network were reported to regulate ECM-receptor interactions (Figure 1C). Subsequently, gene ontology (GO) analysis of these 652 differentially expressed

Table 2. The partially differentially expressed genes in HIV-associated kidney cancer

Gene name	Description	Tumor FPKM	Paracancerous FPKM	log_2FC	p value	Q value
AC079466.1	uncharacterized LOC102724908	13.457	0.011	10.275	0.0001	0.009
CAIX	carbonic anhydrase 9	52.410	0.154	8.407	6.09×10^{-19}	2.23×10^{-14}
NPTX2	neuronal pentraxin 2	125.786	0.705	7.479	1.06×10^{-8}	1.85×10^{-5}
KISS1R	KISS1 receptor	7.172	0.049	7.184	4.17×10^{-8}	5.06×10^{-5}
HOXB13	homeobox B13	1.548	0.011	7.122	0.001	0.036
AF064858.1	novel transcript	6.177	0.062	6.643	8.01×10^{-6}	0.002
PRND	Prion-like protein doppel	5.746	0.063	6.504	6.61×10^{-5}	0.007
IGLON5	IgLON family member 5	1.340	0.016	6.398	2.55×10^{-6}	0.001
AC010655.3	EF-hand calcium binding domain 3 (EFCAB3) pseudogene	24.210	0.293	6.367	1.90×10^{-6}	0.001
TMEM213	transmembrane protein 213 [	2.247	19.460	−3.115	0.006	0.112
AQP2	aquaporin 2	4.075	142.103	−5.124	0.001	0.028
TMEM207	transmembrane protein 207	0.191	7.023	−5.199	1.34×10^{-6}	0.001
FXYD4	FXYD domain containing ion transport regulator 4	1.405	54.209	−5.270	3.42×10^{-5}	0.005
MUC15	mucin 15, cell surface associated	0.174	6.803	−5.293	4.46×10^{-6}	0.001
CLCNKA	chloride voltage-gated channel Ka	1.070	44.995	−5.394	1.43×10^{-6}	0.001
SLC7A13	solute carrier family 7 member 13	0.166	7.516	−5.502	3.92×10^{-5}	0.005
CKM	creatine kinase, M-type	0.025	1.147	−5.507	0.0003	0.016
G6PC	glucose-6-phosphatase catalytic subunit	0.802	36.641	−5.513	3.03×10^{-6}	0.001
TDGF1	teratocarcinoma-derived growth factor 1	0.074	3.633	−5.616	6.68×10^{-8}	6.78×10^{-5}
SIM2	SIM bHLH transcription factor 2	0.112	5.600	−5.645	2.38×10^{-11}	1.09×10^{-7}
SLC12A1	solute carrier family 12 member 1	0.810	54.646	−6.077	6.86×10^{-7}	0.0004
MAB21L4	mab-21-like 4	0.049	3.565	−6.194	3.02×10^{-8}	4.33×10^{-5}
UNCX	UNC homeobox	0.018	1.461	−6.342	5.55×10^{-7}	0.0003
GP2	glycoprotein 2	0.017	2.639	−7.321	1.50×10^{-12}	1.09×10^{-8}
UMOD	uromodulin	4.771	1220.128	−7.999	1.32×10^{-9}	4.00×10^{-6}

(DE)-mRNAs was performed to determine the top 30 GO enrichment categories of these DE-mRNAs in HIV-associated kidney cancer. Several common GO terms were identified for the DE-mRNAs (Figure 1D) in HIV-associated kidney cancer, including vascular endothelial growth factor-activated receptor activity, IgG binding, and lipopolysaccharide receptor activity.

Real-time qPCR validation of DEGs in HIV-associated kidney cancer

Real-time qPCR analyses of KISS1R, CAIX, NPTX2, TMEM213, and UMOD mRNA expression in 18 pairs of HIV-associated kidney cancer and adjacent noncancer tissue samples revealed that 18 of 18 (100.0%) tumors had increased NPTX2 mRNA (110.90-fold) ($p = 0.027$), 13 of 18 (72.2%) tumors had increased KISS1R mRNA (92.08-fold) ($p = 0.020$), and 14 of 18 (77.8%) had increased CAIX mRNA (225.84-fold) ($p = 0.012$) expression in HIV-associated kidney cancer (Figures 2A–2C). In addition, we also found that 15 of 18 (78.6%) tumors had decreased UMOD mRNA (2,308.15-fold) ($p = 0.040$) and 14 of 18 (77.8%) had decreased TMEM213 mRNA (405.95-fold) ($p = 0.037$) expression in HIV-associated kidney cancer (Figures 2D and 2E). To test whether these DEGs were unique to HIV-associated kidney cancer, we analyzed their expression levels in 34 patients with kidney cancer. Thirty-two of 34 (94.1%) tumors had increased NPTX2 mRNA (253.22-fold) ($p = 0.052$), 30 of 34 (88.2%) tumors had increased KISS1R mRNA (94.00-fold) ($p = 0.167$), and 29 of 34 (85.3%) had increased CAIX mRNA (855.56-fold) ($p = 0.058$) expression in kidney cancer (Figures 2F–2H). We also found that 33 of 34 (97.1%) tumors had decreased UMOD mRNA (789.50-fold) ($p < 0.001$) and 31 of 34 (91.2%) had decreased TMEM213 mRNA (893.78-fold) ($p = 0.002$) in kidney cancer (Figures 2I and 2J). Our results indicated that HIV-positive RCC patients were similar to the general population in terms of pathology.

Immunohistochemical staining analysis of KISS1R and CAIX expression in HIV-associated kidney cancer

To investigate the expression of KISS1R and CAIX proteins in benign and malignant kidney tissue, we performed H&E and immunohistochemical (IHC) staining of 18 HIV-associated kidney tumor sample samples (Figure 3). In total, KISS1R- and CAIX-specific staining was clearly observed in the cytoplasm and membrane of primary

Table 3. The Cancer Genome Atlas consortium data on the incidence of genetic alterations of DEGs in HIV-associated kidney cancer based on cancer type

	Kidney renal clear cell carcinoma (n = 392)		Kidney renal clear cell carcinoma (n = 446)		Breast invasive cancer (n = 463)		Bladder urothelial carcinoma (n = 125)		Lung adenocarcinoma (n = 230)	
Gene_symbol	n	%	n	%	n	%	n	%	n	%
CAMK2A	20	**5.1**	66	**14.8**	29	**6.3**	8	**6.4**	1	0.4
STC2	27	**6.9**	75	**16.8**	9	1.9	7	**5.6**	17	**7.4**
FAM153CP	23	**5.9**	69	**15.5**	5	1.1	8	**6.4**	13	**5.7**
COL23A1	23	**5.9**	66	**14.8**	29	**6.3**	8	**6.4**	6	2.6
DPYSL3	23	**5.9**	66	**14.8**	25	**5.4**	8	**6.4**	4	1.7
PCDHB1	21	**5.4**	66	**14.8**	29	**6.3**	7	**5.6**	6	2.6
PCDHGC4	21	**5.4**	70	**15.7**	30	**6.5**	3	2.4	4	1.7
SH3PXD2B	23	**5.9**	65	**14.6**	29	**6.3**	13	**10**	10	4.3
SPARC	21	**5.4**	75	**16.8**	25	**5.4**	5	4.0	4	1.7

[a]Genetic alterations include mutations and/or CNV. Bold values denote the incidence of genetic alterations > 5.0 % [b]The Cancer Genome Atlas Research Network, Nature, 2014, 15.

kidney cancer cells. We observed positive staining of KISS1R and CAIX in HIV-associated kidney ccRcc, SCC, and PRCC (Figure 3). H&E staining of HIV-associated kidney tumors (H&E × 400) showed that the tumor cells of grade I ccRcc in Figure 3A were large with small nuclei, transparent cytoplasm, inconspicuous nucleoli, and no mitosis (red arrow refers to ccRcc). The cells of grade II ccRC in Figure 3D were also large with obvious nucleoli and no mitotic figures. Most of the cells had transparent cytoplasm and some of the cells were eosinophilic small granular cells where the blood vessels were visible in the interstitium (red arrows indicate ccRcc). The tumor cells of grade I–II SCC in Figure 3G were also large and most of the cells were eosinophilic cells with inconspicuous nucleoli and occasional mitotic figures. These cells were arranged in clusters in the stroma (red arrows refers to SCC) (Figure 3G). The cells of grade I PRCC in Figure 3J were medium, papillary shape, cytoplasmic eosinophilia with inconspicuous nucleoli and no mitotic figures (red arrows refer to PRCC tumor cells). Staining of HIV-associated kidney tumors was variable, ranging from cytoplasmic to membranous, with poorly differentiated tumor tissues of ccRcc (grade II) showing higher expression of KISS1R (Figure 3E) and CAIX (Figure 3F) (IHC × 400) compared with the expression of KISS1R (Figure 3B) and CAIX in grade I ccRcc (Figure 3C). We found that KISS1R was almost negatively expressed in grade I ccRcc tumor cells (Figure 3B) but was widely expressed in the cytoplasm of grade II ccRcc and PRCC tumor cells, partly in their nuclear membrane (Figures 3E and 3K). KISS1R also strongly expressed the nuclear membrane of SCC tumor cells and only some of them were expressed in the cytoplasm (Figure 3H). We also found that CAIX was expressed in the cell membrane of grade I ccRcc (Figure 3C) and it was also strongly positively expressed in the nuclear membrane and cytoplasm of grade II ccRcc tumor cells (Figure 3F). Although CAIX was expressed in the cytoplasm of PRCC tumor cells (Figure 3L), weak positive CAIX expression was verified in the cytoplasm of SCC tumor cells (Figure 3I) (IHC × 400). A total of 16 of 18 (88.9%) malignant cases showed positive staining for KISS1R and CAIX. All these results indicated that the expression levels of KISS1R and CAIX are specifically increased in HIV-associated kidney cancer. To better distinguish the kidney cancer tissue from the surrounding tissue, we stained with the kidney cancer cell-specific markers, CD10, CK7, and vimentin and found that 12 of 13 ccRcc cases showed positive staining for CD10 (Figures 4A and 4D) and vimentin (Figures 4C and 4F) and not one of the ccRcc samples was positive for CK7 (Figures 4B and 4E), but CK7 staining was observed in one case of SCC (Figure 4H) and PRCC (Figure 4K).

DISCUSSION

RNA-seq of tumor specimens can help to shed light on the possible pathogenicity of variants of unknown significance because these data provide direct insight into transcriptional alterations and thus improve diagnostic rates.[18] Although we previously identified 758 DEGs in HIV-associated lung cancer and reported that SIX1 and TFAP2A were overexpressed in HIV-associated lung cancer and associated with poorly differentiated tumors,[19] known molecular changes in kidney malignancy among PLWH are limited. This information is important to investigate the molecular mechanisms of HIV-associated kidney cancer. In this study, we first analyzed the baseline characteristics of 18 patients with HIV-associated kidney cancer enrolled in our center. The baseline characteristics of these patients are similar to those of seven patients with HIV-associated RCC enrolled in an Australian statewide HIV center. The median age at RCC diagnosis was 56 years. In addition, six of the seven patients were on ART at RCC diagnosis and five had virological suppression. Two patients had metastatic RCC at diagnosis and the other five patients with clinically localized RCC had radical/partial nephrectomies. The median OS duration of the four patients who died of metastatic RCC was 9 months and the other three patients were alive at a median follow-up of 16 months.[20] These studies suggested that effective biomarkers should be used for the early staging of cancer and personalization of therapy at the time of diagnosis, which may improve HIV-associated kidney cancer patient care. Thus, in our initial biomarker identification stage, transcriptomic sequencing was

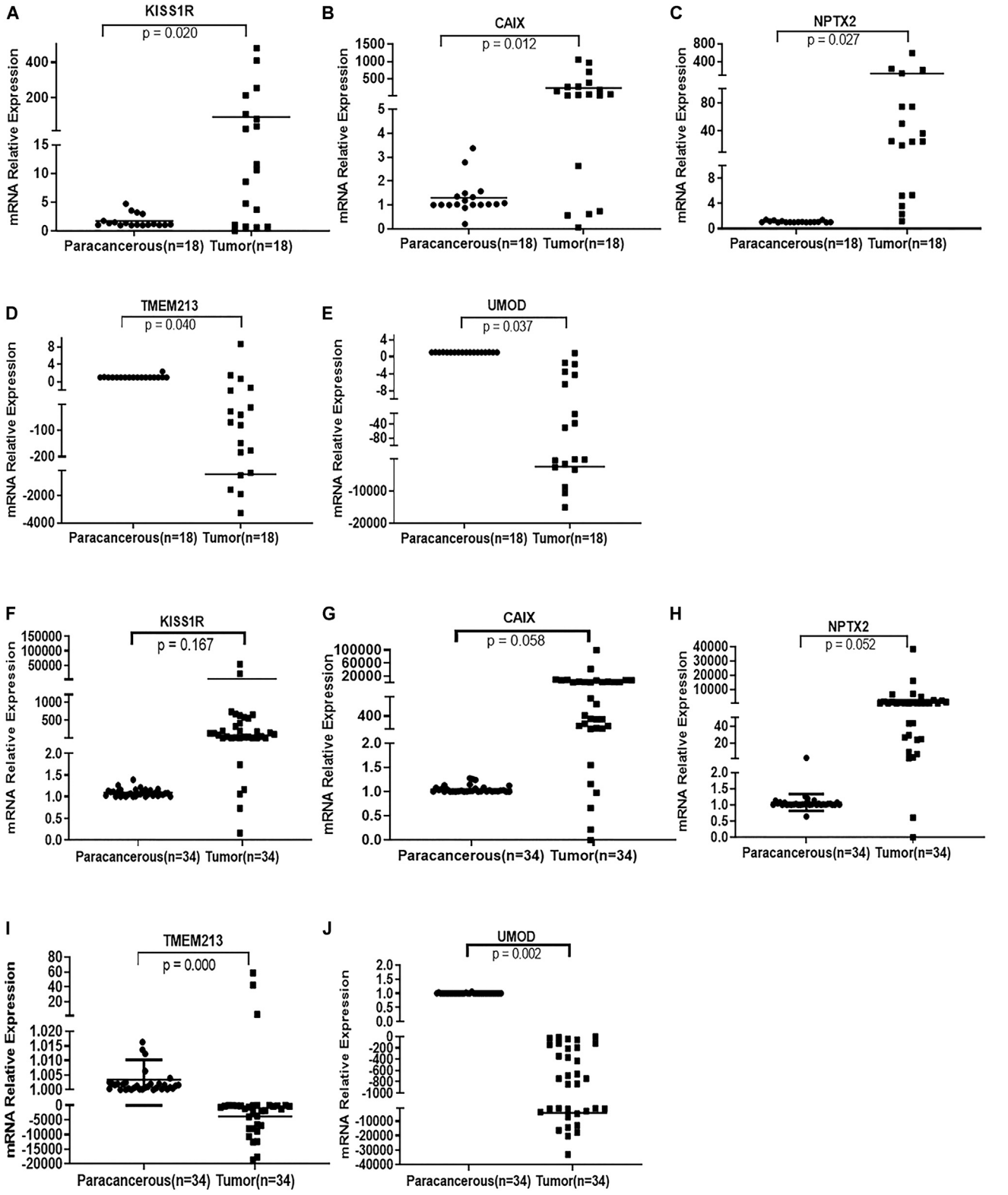

(legend on next page)

performed to assay the DEGs in HIV-associated kidney cancer tumor tissue samples, including seven pairs of tumor/adjacent normal fresh tissue samples. We found that 2,962 protein-coding transcripts, 131 pseudogenes, and 39 novel transcripts were differentially expressed in HIV-associated kidney cancer compared with the adjacent normal tissue groups. Among them, nine DEGs (SLC34A1, STC2, FAM153CP, CDHR2, ACOX2, PCDHB1, CHL1, SLC36A2, and FOXI1) also had a high incidence of genetic alterations in kidney renal clear cell carcinoma in the two kidney cancer TCGA lists of 838 patients.

Next, we identified several pathways from both DE-mRNAs in HIV-associated kidney cancer, including the structure and function of key transporters, tubule and duct development, fructose metabolic processes, and regulation of lipase activity, which may be altered in HIV-associated kidney cancer. Coding variants in apolipoprotein L1 which has broad innate immune functions and can restrict HIV replication *in vitro*, are strongly associated with HIV-associated nephropathy in persons with untreated HIV infection.[21] Strong associations in genome-wide association studies were noted between chronic kidney disease and UMOD promoter variants, which influenced urinary uromodulin levels.[22] Uromodulin encoded by UMOD can be secreted and passively excreted in urine.[23] Several TMEM family members were deregulated in ccRcc tumors as components of cellular membranes (such as mitochondrial membranes, ER, lysosomes, and Golgi apparatus), suggesting their importance in the pathogenesis of ccRcc with the involvement of ER proteins.[24] Our real-time qPCR analyses also validated that TMEM213 and UMOD were repressed in HIV-associated kidney cancer (Figures 2A–2E) and that KISS1R, CAIX, and NPTX2 were significantly upregulated in HIV-associated kidney cancer ($p < 0.05$) (Figures 2A–2C). Positive staining for KISS1R and CAIX was further observed in HIV-associated kidney ccRcc (Figures 3C, 3E, and 3F) SCC (Figures 3H and 3I), and PRCC (Figures 3K and 3L). The DEGs CAIX, NPTX2, and UMOD were also found in the formalin-fixed, paraffin-embedded (FFPE) and RNAlater datasets and confirmed by immunohistochemistry.[25] More importantly, we found higher expression of KISS1R (Figure 3E) and CAIX in the tumor tissues of grade II ccRcc (Figures 3E and 3F) compared with KISS1R and CAIX expression in grade I ccRcc (Figures 3B and 3C), which demonstrated that increased KISS1R and CAIX expression was closely linked to poor clinical prognosis of cancer patients. Cytokeratin (CK) AE1/AE3 and vimentin immunoexpression were also analyzed in 26 CCRCCs. CK AE1/AE3 immunoexpression was associated with low-grade and early-stage lesions. Vimentin immunoexpression was also associated with high-grade and advanced lesions.[26] In clear cell RCC, 89.2% of cancers showed strong positivity for CAIX staining. The frequency and intensity of CAIX staining varied between different RCC tumor types and CAIX staining was strong in 61.2% of 1,677 tumor tissue samples.[27] On the other hand, the KISS1 protein can be rapidly processed in serum into smaller but biologically active peptides called kisspeptins through the G-protein-coupled receptor KISS1R. KISS1, kisspeptins, and KISS1R might regulate the development and progression of several cancers, including melanoma and pancreatic, colorectal, bladder, and ovarian cancer.[28] Although high expression of KISS1R and CAIX was associated with poor OS in oral tongue SCC,[29] the OS did not differ by the expression levels of KISS1R and CAIX among the 18 patients with HIV-associated kidney cancer, possibly because of the small sample size (Figure S1). We also analyzed KISS1R, CAIX, NPTX2, TMEM213, and UMOD expression in 34 pairs of kidney tumors compared with adjacent noncancer tissue samples from the general kidney cancer population and revealed that the expression levels of KISS1R ($p = 0.167$), CAIX ($p = 0.058$), and NPTX2 ($p = 0.052$) were not significantly increased in kidney tumor tissue from the general kidney cancer population. Our study aims to heighten the awareness of kidney cancer occurring in HIV/AIDS while highlighting some of the clinical features to facilitate early recognition and diagnosis In this study we reveal the molecular changes in kidney malignancy among PLWH. Our data suggest that certain DEGs play key roles in kidney malignancy and may represent novel biomarkers for HIV-associated kidney cancer. Thus, the molecular changes we have identified in kidney malignancy can offer the hope of early detection as well as tracking disease progression and recurrence. Understanding the mechanisms underlying kidney malignancies in HIV infection may also help to improve treatment of the growing population of HIV patients.

Finally, the limitations of this study should be noted. Our current sample size of patients with non-HIV kidney cancer or HIV-associated kidney cancer is small. The limitations of this study are that the lack of tissue for comparison limits the ability to determine the specificity of differential gene expression for HIV-infected kidney cancer. It would be interesting to find other DEGs or pathways in HIV-infected kidney cancer that are specific to HIV. Against this background, there is an opportunity to develop novel gene signatures for HIV-associated cancer that are useful for the early detection of HIV-associated kidney cancer. This study is notable because the information reported herein may be useful for early detection as well as tracking disease progression and recurrence, which would help kidney cancer screening in HIV-infected populations and guide treatment of this disease.

MATERIALS AND METHODS

Patients and tissue specimens

A total of 18 patients presenting at the Shanghai Public Health Clinical Center (Shanghai, China) were diagnosed with HIV-associated kidney cancer from March 2014 to May 2019. The ages of the

Figure 2. Real-time qPCR analysis of KISS1R, CAIX, NPTX2, TMEM213, and UMOD mRNA expression in 18 pairs of HIV-associated kidney cancer and adjacent noncancer tissue samples and 34 pairs of kidney cancer and adjacent noncancer tissue samples (Cont, adjacent noncancer tissue; Ca, kidney tumor tissue)

(A–E) HIV-associated kidney tumor and adjacent noncancer tissue samples; (F–J) kidney tumor and adjacent noncancer tissue samples; (A and F) KISS1R; (B and G) CAIX; (C and H) NPTX2; (D and I) TMEM213; (E and J) UMOD.

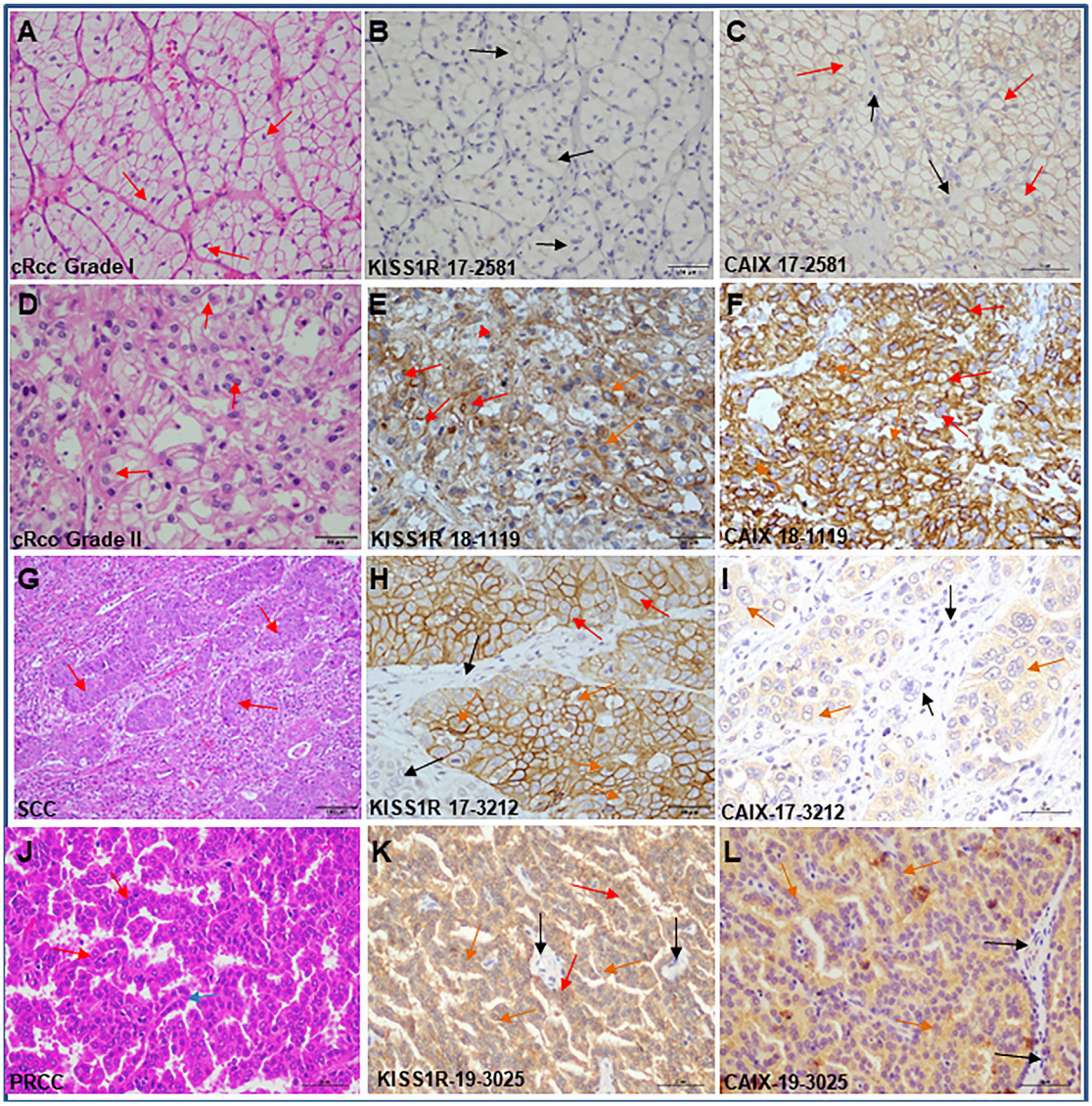

Figure 3. Immunohistochemical analysis of KISS1R and CAIX protein expression in HIV-associated kidney tumor tissue samples

H&E staining of kidney tumor tissue samples (A, D, G, and J). Staining of variably differentiated kidney tumor samples with an anti-KISS1R antibody (B, E, H, and K) and an anti-CAIX antibody (C, F, I, and L) (Red arrows refer to KISS1R/CAIX expressed in the cell membrane or nuclear membrane; orange arrows refer to KISS1R/CAIX expressed in the cell cytoplasm; and black arrows indicate negative KISS1R/CAIX expression; IHC × 400).

18 patients with HIV-associated kidney cancer varied from 24 to 65 years (median, 51 years). The clinicopathological features of the patients included age at diagnosis, sex, cigarette smoking, complications, HAART treatment, $CD4^+$ count, surgical approach, pathological type, and TNM stage. Written informed consent was obtained from all patients for the use of tissue samples and clinical records. The study protocol was performed under approval of the Ethics Committee of Shanghai Public Health Clinical Center. All cases were evaluated by two staff pathologists (Dr. J. Xu and Dr. Y. Feng) who were blinded to the clinical outcome and follow-up data.

RNA purification, whole-transcriptome library construction, and sequencing

RNA was purified from 18 HIV-associated kidney cancer tumor/adjacent normal tissue samples using TRIzol LS reagent (Invitrogen, Carlsbad, CA, USA) and the RNAsimple total RNA kit (Tiangen Biotech, Beijing, China). The quality of the purified RNA was assessed using an Agilent 2100 Bioanalyzer (Agilent Technologies, Waldbronn, DE, USA). RNA from HIV-associated kidney tumor tissue samples, including seven pairs of tumor/adjacent normal fresh tissue samples, was used for transcriptomic sequencing. Paired-end libraries

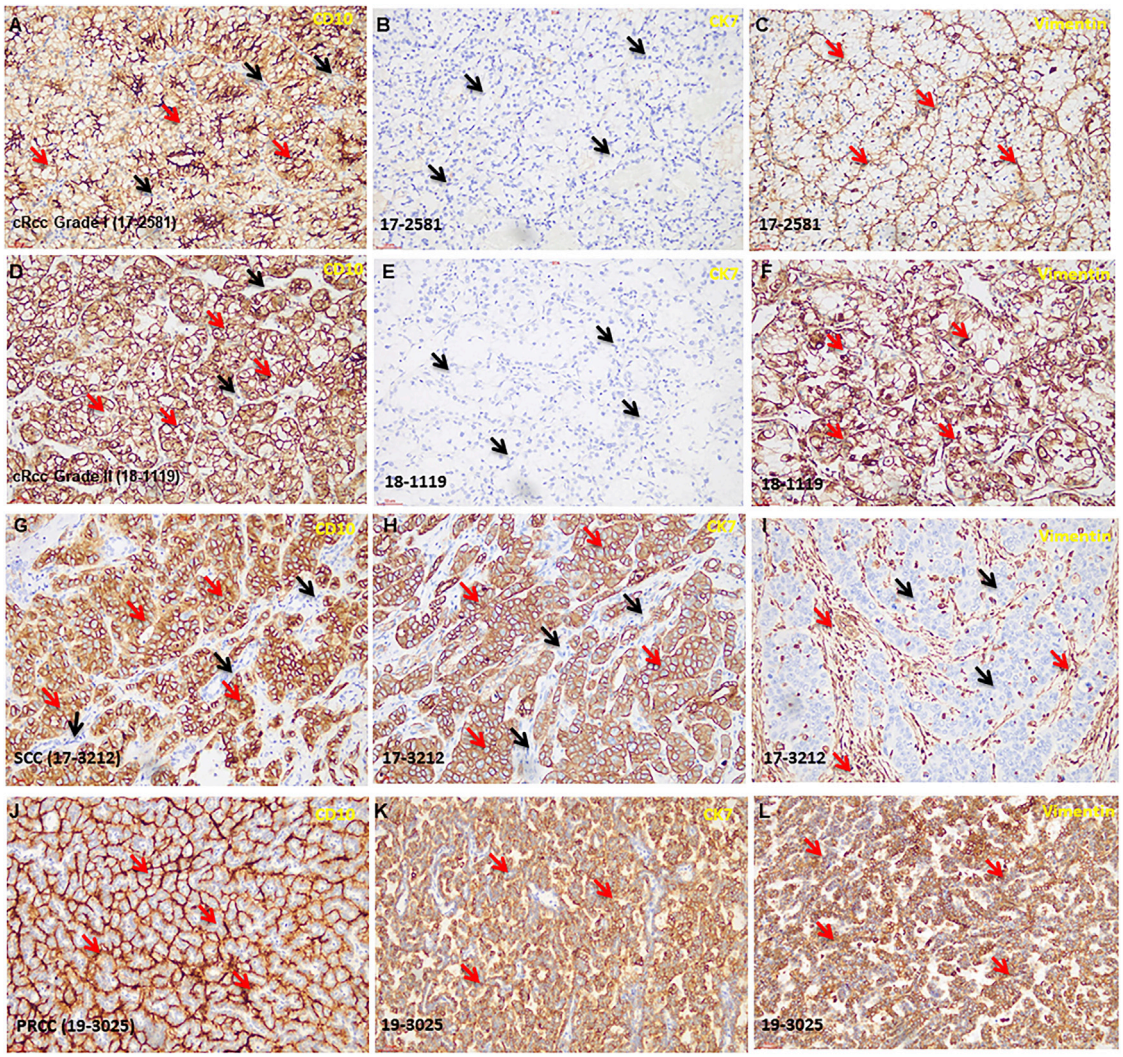

Figure 4. Immunohistochemical analysis of CD10, CK7 and Vimentin protein expression in HIV-associated kidney tumor tissue samples

Staining with anti-CD10 (A, D, G, and J), anti-CK7 (B, E, H, and K), and anti-vimentin antibodies (C, F, I, and L). (Red arrows refer to CD10/CK7/vimentin expression; black arrows indicate negative CD10/CK7/vimentin expression; IHC × 400).

were synthesized using the TruSeq RNA Sample Preparation Kit (Illumina, USA). After poly-A-containing mRNA molecules were purified using poly-T oligo-attached magnetic beads, the mRNA was fragmented into small pieces using divalent cations at 94°C for 8 min. The cleaved RNA fragments were copied into first-strand cDNA using reverse transcriptase and random primers. Then, the second strand of cDNA was synthesized using DNA polymerase I and RNase H. These cDNA fragments then underwent an end repair process with the addition of a single "A" base and the ligation of the adapters. The products were then purified and enriched by PCR to create the final cDNA library. Afterward, the purified libraries were quantified using a Qubit 2.0 Fluorometer (Life Technologies, USA) and validated using an Agilent 2100 Bioanalyzer. The library was sequenced on an Illumina NovaSeq 6000 (Illumina). All library construction and sequencing were performed at Sinotech Genomics (Shanghai, China) according to Affymetrix (Santa Clara, CA, USA) protocol.

RNA-seq data analysis and functional annotation

Paired-end sequence files (fastq) were aligned to hg38 using Hisat2 (Hierarchical Indexing for Spliced Alignment of Transcripts, version 2.0.5) as described previously.[30] The output SAM (sequencing alignment/map) files were converted to BAM (binary alignment/map) files and sorted using SAMtools (version 1.3.1). Gene abundance was expressed as fragments per kilobase of exon per million reads mapped (FPKM). StringTie software was used to count the fragment within each gene and the TMM algorithm was used for normalization. Differential expression analysis for mRNA in HIV-associated kidney

cancer was performed using the R package edgeR, which applies a series of statistical methodology based on the negative binomial distributions (empirical Bayes estimation, exact tests, and quasi-likelihood tests). Differentially expressed RNAs with $|\log_2(FC)| > 1$, $q < 0.051$, and $q < 0.05$, and one group's mean FPKM > 1, considered significantly modulated, were retained for further analysis. To identify potential specific pathways based on changes in gene expression, GO annotation and enrichment were conducted based on the GO database (http://www.geneontology.org/). GO-enriched items are shown, and corrected Q values <0.05 were considered significant. Significantly enriched pathways and biological processes were displayed with R software as described previously.[31]

cBioPortal analysis of TCGA data of multiple types of cancer to determine the probability of gene expression alteration and protein-protein interaction network analysis

We investigated our candidate genes using cBioPortal analysis of TCGA data via cBioPortal [19] and generated the probability of DEGs for four different types of cancers: kidney renal clear cell carcinoma (TCGA, Nature 2013, n = 392; TCGA, Firehose Legacy, n = 446), breast invasive carcinoma (TCGA, Nature 2012, n = 463), bladder urothelial carcinoma (TCGA, Nature 2014, n = 125), and lung adenocarcinoma (TCGA, Nature 2014, n = 230). Next, to explore the interaction of DE-mRNAs of HIV-associated kidney cancer, DE-mRNA lists were first imported into the STRING database (https://string-db.org) and a protein-protein interaction (PPI) network was generated. When constructing the PPI network, PPI pairs with a medium confidence of interaction score >0.9 were exported.

Real-time qPCR analysis

Total RNA (1 μg) was reverse transcribed to cDNA using the PrimeScript RT reagent kit with gDNA Eraser (cat. no. RR047A, TaKaRa, Shiga, Japan). Real-time qPCR was performed using a LightCycler 480 II instrument (Roche Molecular Systems) and TB Green Premix Ex Taq II (Tli RNase H Plus) (cat. no. RR820A, TaKaRa). qPCR results were analyzed using LightCycler 480 Software version 1.5 (Roche Molecular Systems) and normalized using 18S ribosomal RNA. Eighteen pairs of HIV-associated kidney cancer and adjacent noncancer tissue samples were used for real-time qPCR analysis. The specific primers of the mRNAs are presented in Table S1.

IHC staining

IHC staining for KISS1R and CA9 was performed using 18 FFPE tissue samples from the Shanghai Public Health Clinical Center, Fudan University. Paraffin-embedded tissues were dewaxed in xylene, rehydrated by serial concentrations of ethanol, rinsed in phosphate-buffered saline (PBS) and then treated with 3% H_2O_2. After being heated at 60°C overnight, the sections were incubated with 10% normal goat serum at room temperature for 10 min. This step was followed by a PBS wash and incubation with anti-KISS1R (cat. no. YT2480, Immunoway, Plano, TX, USA) or anti-CAIX (cat. no. YM3076, Immunoway) antibodies for 12 h at 4°C followed by horseradish peroxidase-conjugated goat anti-rabbit IgG (1/500; Invitrogen, Thermo Fisher Scientific). After a PBS wash, the sections were developed in DAB substrate. The sections were then counterstained in hematoxylin for 2 min and dehydrated in ethanol and xylene before being mounted. Eighteen paraffin-embedded tissues were retrieved for IHC analysis. Staining patterns, including cell distribution (membrane, cytoplasmic, and nuclear pattern) and the extent and intensity of staining, were evaluated independently for each specimen by two investigators. For CALX and KISS1R, a 0–4 scale was used for evaluation as follows: negative, focal (<10%), regional (10–50%), and diffuse (>50%). Tumors presenting regional and diffuse staining were considered positive, and tumors with negative or patchy staining were categorized as negative.

Statistical analysis

Data analyses were performed using SPSS statistical package 17.0 (SPSS, Chicago, IL, USA). Statistical values are presented as the means ± standard deviations. Student's t test was used to assess differences between groups. Univariate analysis was performed using the Kaplan-Meier estimator method and a log rank test. The median survival time was calculated using SPSS. $p < 0.05$ was considered to indicate a statistically significant difference.

Data availability statement

The complete RNA-seq datasets of HIV-associated kidney cancer were deposited in the Gene Expression Omnibus database under accession number GSE205204.

SUPPLEMENTAL INFORMATION

Supplemental information can be found online at https://doi.org/10.1016/j.omtn.2022.06.002.

ACKNOWLEDGMENTS

This research was supported by a grant from the Science and Technology Commission of Shanghai (20Y11900700), a grant from the Shanghai Natural Science Foundation (20ZR1470500), a grant from the Special Research Fund of Youan Medical Alliance for the Liver and Infectious Diseases (LM202020), and a grant (KY-GW-2020-09) (to X.H.) from Shanghai Public Health Clinical Center, Shanghai, China. The authors also want to thank Miss Xiaoxiao Sun (Sinotech Genomics, Shanghai, China) for the technical support for RNA-seq data analysis.

AUTHOR CONTRIBUTIONS

J.W. and J.B. conceived and designed the study. J.B. and J.Y. collected the clinic kidney tumor samples. J.X., L.W., and Q.L. analyzed the data. J.Y., X.Z., and J.X. collected the literature. J.W. and J.B. wrote the manuscript. J.W., S.L., L.W., Z.L., F.L., X.H., H.Z., Y.F., C.C., and T.Z. revised the manuscript. J.W. and J.X. provided funding support.

DECLARATION OF INTERESTS

The authors declare no competing interests.

REFERENCES

1. Coghill, A.E., Pfeiffer, R.M., Shiels, M.S., and Engels, E.A. (2017). Excess mortality among HIV-infected individuals with cancer in the United States. Cancer Epidemiol. Biomarkers Prev. *26*, 1027–1033. https://doi.org/10.1158/1055-9965.epi-16-0964.
2. Engels, E.A., Biggar, R.J., Hall, H.I., Cross, H., Crutchfield, A., Finch, J.L., Grigg, R., Hylton, T., Pawlish, K.S., McNeel, T.S., and Goedert, J.J. (2008). Cancer risk in people infected with human immunodeficiency virus in the United States. Int. J. Cancer *123*, 187–194. https://doi.org/10.1002/ijc.23487.
3. Coghill, A.E., Han, X., Suneja, G., Lin, C.C., Jemal, A., and Shiels, M.S. (2019). Advanced stage at diagnosis and elevated mortality among US patients with cancer infected with HIV in the National Cancer Data Base. Cancer *125*, 2868–2876. https://doi.org/10.1002/cncr.32158.
4. Franzetti, M., Ricci, E., and Bonfanti, P. (2019). The pattern of non-AIDS-defining cancers in the HIV population: epidemiology, risk factors and prognosis. A review. Curr. HIV Res. *17*, 1–12. https://doi.org/10.2174/1570162x17666190327153038.
5. Smith, C.J., Ryom, L., Weber, R., Morlat, P., Pradier, C., Reiss, P., Kowalska, J.D., de Wit, S., Law, M., el Sadr, W., et al. (2014). Trends in underlying causes of death in people with HIV from 1999 to 2011 (D:A:D): a multicohort collaboration. Lancet *384*, 241–248. https://doi.org/10.1016/s0140-6736(14)60604-8.
6. Althoff, K.N., Gebo, K.A., Moore, R.D., Boyd, C.M., Justice, A.C., Wong, C., Lucas, G.M., Klein, M.B., Kitahata, M.M., Crane, H., et al. (2019). Contributions of traditional and HIV-related risk factors on non-AIDS-defining cancer, myocardial infarction, and end-stage liver and renal diseases in adults with HIV in the USA and Canada: a collaboration of cohort studies. Lancet HIV *6*, e93–e104. https://doi.org/10.1016/s2352-3018(18)30295-9.
7. Adih, W.K., Selik, R.M., and Hu, X. (2011). Trends in diseases reported on US death certificates that mentioned HIV infection, 1996-2006. J. Int. Assoc. Phys. AIDS Care *10*, 5–11. https://doi.org/10.1177/1545109710384505.
8. Selik, R.M., Byers, R.H., Jr., and Dworkin, M.S. (2002). Trends in diseases reported on U.S. death certificates that mentioned HIV infection, 1987-1999. J. Acquir. Immune Defic. Syndr. *29*, 378–387. https://doi.org/10.1097/00126334-200204010-00009.
9. Avettand-Fènoël, V., Hocqueloux, L., Ghosn, J., Cheret, A., Frange, P., Melard, A., Viard, J.P., and Rouzioux, C. (2016). Total HIV-1 DNA, a marker of viral reservoir dynamics with clinical implications. Clin. Microbiol. Rev. *29*, 859–880. https://doi.org/10.1128/cmr.00015-16.
10. Avettand-Fenoël, V., Rouzioux, C., Legendre, C., and Canaud, G. (2017). HIV infection in the native and allograft kidney: implications for management, diagnosis, and transplantation. Transplantation *101*, 2003–2008. https://doi.org/10.1097/tp.0000000000001674.
11. Swanepoel, C.R., Atta, M.G., D'Agati, V.D., Estrella, M.M., Fogo, A.B., Naicker, S., Post, F.A., Wearne, N., Winkler, C.A., Cheung, M., et al. (2018). Kidney disease in the setting of HIV infection: conclusions from a kidney disease: improving global outcomes (KDIGO) controversies conference. Kidney Int. *93*, 545–559. https://doi.org/10.1016/j.kint.2017.11.007.
12. Zhang, M., Zhu, Z., Xue, W., Liu, H., and Zhang, Y. (2021). Human immunodeficiency virus-related renal cell carcinoma: a retrospective study of 19 cases. Infect. Agents Cancer *16*, 26. https://doi.org/10.1186/s13027-021-00362-7.
13. Li, M., Wang, Y., Cheng, L., Niu, W., Zhao, G., Raju, J.K., Huo, J., Wu, B., Yin, B., Song, Y., and Bu, R. (2017). Long non-coding RNAs in renal cell carcinoma: a systematic review and clinical implications. Oncotarget *8*, 48424–48435. https://doi.org/10.18632/oncotarget.17053.
14. Grulich, A.E., van Leeuwen, M.T., Falster, M.O., and Vajdic, C.M. (2007). Incidence of cancers in people with HIV/AIDS compared with immunosuppressed transplant recipients: a meta-analysis. Lancet *370*, 59–67. https://doi.org/10.1016/s0140-6736(07)61050-2.
15. Chen, C.H., Chung, C.Y., Wang, L.H., Lin, C., Lin, H.L., and Lin, H.C. (2015). Risk of cancer among HIV-infected patients from a population-based nested case-control study: implications for cancer prevention. BMC Cancer *15*, 133. https://doi.org/10.1186/s12885-015-1099-y.
16. Isaguliants, M., Bayurova, E., Avdoshina, D., Kondrashova, A., Chiodi, F., and Palefsky, J.M. (2021). Oncogenic effects of HIV-1 proteins, mechanisms behind. Cancers *13*, 305.
17. Durinck, S., Stawiski, E.W., Pavía-Jiménez, A., Modrusan, Z., Kapur, P., Jaiswal, B.S., Zhang, N., Toffessi-Tcheuyap, V., Nguyen, T.T., Pahuja, K.B., et al. (2015). Spectrum of diverse genomic alterations define non-clear cell renal carcinoma subtypes. Nat. Genet. *47*, 13–21. https://doi.org/10.1038/ng.3146.
18. Kremer, L.S., Bader, D.M., Mertes, C., Kopajtich, R., Pichler, G., Iuso, A., Haack, T.B., Graf, E., Schwarzmayr, T., Terrile, C., et al. (2017). Genetic diagnosis of Mendelian disorders via RNA sequencing. Nat. Commun. *8*, 15824. https://doi.org/10.1038/ncomms15824.
19. Zheng, J., Wang, L., Cheng, Z., Pei, Z., Zhang, Z., Li, Z., Zhang, X., Yan, D., Xia, Q., Feng, Y., et al. (2018). Molecular changes of lung malignancy in HIV infection. Sci. Rep. *8*, 13128. https://doi.org/10.1038/s41598-018-31572-6.
20. Ong, W.L., King, K., Koh, T.L., Chipman, M., Royce, P., Hoy, J., and Millar, J.L. (2016). HIV and renal cell carcinoma: experience in an Australian statewide HIV center. Asia Pac. J. Clin. Oncol. *12*, 188–193. https://doi.org/10.1111/ajco.12487.
21. An, P., Kirk, G.D., Limou, S., Binns-Roemer, E., Kopp, J.B., and Winkler, C.A. (2019). Impact of APOL1 genetic variants on HIV-1 infection and disease progression. Front. Immunol. *10*, 53. https://doi.org/10.3389/fimmu.2019.00053.
22. Olden, M., Corre, T., Hayward, C., Toniolo, D., Ulivi, S., Gasparini, P., Pistis, G., Hwang, S.J., Bergmann, S., Campbell, H., et al. (2014). Common variants in UMOD associate with urinary uromodulin levels: a meta-analysis. J. Am. Soc. Nephrol. *25*, 1869–1882. https://doi.org/10.1681/asn.2013070781.
23. Belliere, J., Faguer, S., Huart, A., Ribes, D., Chassaing, N., Roussel, M., and Chauveau, D. (2019). UMOD genetic variations and myeloma cast nephropathy. Clin. Kidney J. *12*, 639–640. https://doi.org/10.1093/ckj/sfz071.
24. Wrzesiński, T., Szelag, M., Cieślikowski, W.A., Ida, A., Giles, R., Zodro, E., Szumska, J., Poźniak, J., Kwias, Z., Bluyssen, H.A., and Wesoly, J. (2015). Expression of pre-selected TMEMs with predicted ER localization as potential classifiers of ccRCC tumors. BMC Cancer *15*, 518. https://doi.org/10.1186/s12885-015-1530-4.
25. Eikrem, O., Beisland, C., Hjelle, K., Flatberg, A., Scherer, A., Landolt, L., Skogstrand, T., Leh, S., Beisvag, V., and Marti, H.P. (2016). Transcriptome sequencing (RNAseq) enables utilization of formalin-fixed, paraffin-embedded biopsies with clear cell renal cell carcinoma for exploration of disease biology and biomarker development. PLoS One *11*, e0149743. https://doi.org/10.1371/journal.pone.0149743.
26. Stepan, A.E., Mărgăritescu, C., Stoica, L.E., Stepan, M.D., and Simionescu, C.E. (2018). Clear cell renal cell carcinomas - epithelial and mesenchymal immunophenotype. Rom. J. Morphol. Embryol. *59*, 1189–1194.
27. Büscheck, F., Fraune, C., Simon, R., Kluth, M., Hube-Magg, C., Möller-Koop, C., Shadanpour, N., Bannenberg, C., Eichelberg, C., Höflmayer, D., et al. (2018). Aberrant expression of membranous carbonic anhydrase IX (CAIX) is associated with unfavorable disease course in papillary and clear cell renal cell carcinoma. Urol. Oncol. *36*, 531.e19–531.e25. https://doi.org/10.1016/j.urolonc.2018.08.015.
28. Guzman, S., Brackstone, M., Radovick, S., Babwah, A.V., and Bhattacharya, M.M. (2018). KISS1/KISS1R in cancer: friend or foe? Front. Endocrinol. *9*, 437. https://doi.org/10.3389/fendo.2018.00437.
29. Wang, S., Fu, Z., Wang, Y., Sun, Y., Cui, L., Wang, C., Liu, Q., Shao, D., Wang, Y., and Wen, N. (2020). Correlation of carbonic anhydrase 9 (CA9) with pathological T-stage and prognosis in patients with oral tongue squamous cell carcinoma. Ann. Transl. Med. *8*, 1521. https://doi.org/10.21037/atm-20-7144.
30. Huang, S., Liu, D., Sun, J., Zhang, H., Zhang, J., Wang, Q., Gan, L., Qu, G., Qiu, J., Deng, J., et al. (2022). Tim-3 regulates sepsis-induced immunosuppression by inhibiting the NF-κB signaling pathway in CD4 T cells. Mol. Ther. *30*, 1227–1238. https://doi.org/10.1016/j.ymthe.2021.12.013.
31. Jia, N., Tong, H., Zhang, Y., Katayama, H., Wang, Y., Lu, W., Zhang, S., and Wang, J. (2019). CeRNA expression profiling identifies KIT-related circRNA-miRNA-mRNA networks in gastrointestinal stromal tumour. Front. Genet. *10*, 825. https://doi.org/10.3389/fgene.2019.00825.